

A Study of the Hydrogen Pre-treatment of Gallium and Platinum Promoted ZSM-5 in Ethane Dehydroaromatization

Ashley Caiola ^a, Brandon Robinson ^a, Xinwei Bai ^a, Dushyant Shekhawat ^b and Jianli Hu ^a

^a Department of Chemical and Biomedical Engineering, West Virginia University, Morgantown, WV, 26505

^b National Energy Technology Laboratory, U.S. Department of Energy, 3610 Collins Ferry Rd. Morgantown, WV, 26505

Keywords: Catalysis, Dehydroaromatization, Pyridine DRIFTS, and Natural Gas

Abstract

The performances of gallium and platinum promoted ZSM-5 catalysts, fresh and reduced, were studied for the dehydroaromatization of ethane to aromatics. Fresh and reduced 2% Ga/ZSM-5, 1.5% Ga-0.5% Pt/ZSM-5, and 0.5% Pt/ZSM-5 were tested in a fixed-bed reactor system at 615°C for 2-hrs time on stream. It was observed that the hydrogen reduction of the fresh Pt containing catalysts led to an increase in catalytic conversion. The addition of platinum to the gallium catalyst resulted in an increase in the reducibility of the Ga species on the surface of the zeolite. The GaPt catalysts exhibited an increase in ethane conversion and the stability of aromatic production selectivity over the Ga and Pt catalysts. The as-prepared fresh catalysts were characterized by ICP and BET. The fresh and reduced catalysts were further analyzed by XRD, H₂-TPR, XPS, pyridine-DRIFTS, TGA and TEM.

1. Introduction

The world's demand for natural gas has been growing consistently over the past few decades. Natural gas is considered a potential alternative to oil and coal because of its ability to burn cleaner. Although not completely emission free, it has dominated the energy industry by providing a continuous supply of cheap fuel. Currently, natural gas makes up 41% of North American energy production.¹ The conversion of natural gas to value-added chemicals, typically involves the indirect production of synthesis gas (syngas) as an intermediate before the production of the desired product. Steam reforming and partial oxidation are two of the most common indirect methods of natural gas conversion. Steam reforming is the production of syngas by reacting steam (water) with natural gas at high temperatures. Partial oxidation also produces a lower quantity of syngas than steam reforming by reacting oxygen with natural gas. However, both involve the intermediate synthesis of syngas, which causes these processes to be both energy and capital intensive.²⁻⁶ Alternatively, the direct conversion of light alkanes, such as methane and ethane, into aromatics eliminates the expensive intermediate production of syngas and the greenhouse gas CO₂ emissions from steam reforming.^{2,7} This topic has been heavily investigated over the past few decades due to its importance in the production of value-added chemicals and fuels. Ethane is the second-largest component of natural gas that is often used as a feedstock in the catalytic natural gas dehydroaromatization (DHA) reaction, similarly to methane. Although the conversion of natural gas by the direct method shows promise as a cost-efficient approach, the commercialization of this process faces some obstacles. The main technical challenges are related to low selectivity, catalyst coking, deactivation, and regeneration. The accumulation of carbon on the catalyst's surface can block the active sites, therefore resulting in a decrease in the activity or deactivation of the catalyst over time.⁶⁻¹¹

The use of zeolite-supported metal catalysts in the transformation of light alkanes to aromatics has been studied for decades. The catalysts performance, activity, and product selectivity depend on the choice and composition of the transition-metal promoter(s). Over the past decades, researchers have explored the use of Mo, Fe, Zn, Re, Co, Ga, Pt, along with many others as the active metal species in the direct transformation of ethane to aromatics.^{6, 11-20} Among the many options, Ga and Pt have shown increased promise as promoters. Ga has shown promise as a promoter due to its excellent ability in the dehydrogenation step of propane DHA.²¹ Sattler et al. had shown that the addition of Pt to Ga/Al₂O₃ resulted in a highly active, selective, and stable catalyst for propane dehydrogenation.²² Pt-based catalysts have widely been used for the dehydrogenation of alkanes, such as methane, ethane, propane, and butane.^{10, 12} Reschetilowski et al. showed the influence of platinum dispersion and metal particle size distribution in the catalytic activity of a Pt/HZSM-5 catalyst for ethane aromatization. They suggested that well-dispersed Pt particles on the catalyst can help facilitate the aromatization of ethane.²³

Zeolites have been extensively researched and optimized for a wide variety of applications over many decades. They have been used in many industrial processes in oil refineries, biomass conversion, direct valorization of natural gas and more.²⁴ The zeolite's framework provides a unique shape-selective channel which can be optimized for a specific application or reaction. The zeolite, ZSM-5, is an aluminosilicate material with an inverted mordenite framework (MFI).²⁵⁻²⁹ MFI type zeolites are composed of pentasil units which are linked to form pentasil chains. Oxygen bridges connect these chains to form corrugated sheets, each sheet is then connected by oxygen bridges to the next to form a three-dimensional 10-ring channel system containing micropores of about 0.55 nm. The micropore size of ZSM-5 is optimal for the dynamic molecular sizes of the BTX aromatics (benzene, toluene, and xylene). The MFI type zeolites pores are large enough for the BTX to diffuse out but small enough to hinder polyaromatic species growth within the pores. These unique features make the ZSM-5 an ideal support for the direct conversion of light alkanes to aromatics.^{17, 24-26, 28-29} Zeolites can be categorized by what is known as a SiO₂/Al₂O₃ ratio (SAR), which can influence the zeolites acidity, catalytic activity, hydrophobic/hydrophilic behavior, and polarization towards reactants and products.^{30, 31}

The surface acidity of zeolites has been extensively researched to determine the type, strength, and the number of acid sites, which can affect the zeolite supports potential catalytic performance.^{25, 32-36} Characterization of these sites is important, so a variety of physiochemical techniques have been developed over the years. The use of a gaseous probe molecule to inspect the adsorption-desorption processes is very commonly used by researchers. This technique is often combined with the gravimetric or thermal desorption measurements and spectroscopic measurements (IR).^{25, 32, 33} Ammonia temperature programmed desorption (TPD) investigates the adsorption and desorption profile of ammonia on the surface acid sites of the zeolite structure.³⁴ Infrared spectroscopy is a powerful characterization tool used to determine structural information about the zeolite lattice from its vibrational frequencies. The position of bands is respective to the typical adsorption sites on the zeolite's surface. For ZSM-5, information about the Brönsted acid sites is associated with the bands around 1540cm⁻¹, whereas the Lewis acid sites give rise to bands around 1450cm⁻¹. The band at 1490 cm⁻¹ has been attributed to a combination of both Brönsted and Lewis acid sites.^{25, 32, 35, 36} It is commonly accepted throughout literature that the first step of ethane dehydroaromatization is the dehydrogenation of ethane to ethylene. This step has been shown to be promoted by the metal sites on the zeolite

catalysts.^{17, 18, 35, 37} Following the dehydrogenation of ethane the second step is considered to be the oligomerization of olefins, cyclization, and final dehydrogenation to aromatics. The oligomerization of the olefins has been shown to occur on the Brönsted acid sites of the metal promoted zeolite catalyst.^{17, 18, 35, 37} Specifically it has been shown for Ga-modified ZSM-5 that the intra-zeolite Ga species of the catalyst can dehydrogenate ethane to form ethylene, which then can be further oligomerized and aromatized by the Ga Lewis acid sites species and the Brönsted acid sites.^{35, 37, 38}

In this work, the effectiveness of the hydrogen pre-treatment of gallium and platinum promoted ZSM-5 was tested for the ethane dehydroaromatization reaction. The effects of each promoter individually and combined were examined for catalytic conversion and product distribution. The as-prepared fresh catalysts were characterized by ICP and BET. The fresh and reduced catalysts were further analyzed by XRD, H₂-TPR, XPS, and pyridine-DRIFTS to elucidate the active metal species and the acidity of the zeolite surface prior to the ethane DHA reaction. The spent fresh and reduced catalysts were characterized using TGA/DTA and TEM, to determine the effect of the reaction on the catalysts.

2. Methods & Materials

2.1. Catalyst Preparation

The ammonium form of the ZSM-5 zeolite (NH₄-ZSM-5) was purchased from Zeolyst International with a SiO₂/Al₂O₃ mole ratio (SAR) of 23. The metal precursor gallium nitrate hydrate Ga(NO₃)₃·xH₂O, and chloroplatinic acid hexahydrate H₂PtCl₆·6H₂O, were purchased from Alfa Aesar. The NH₄-ZSM-5 zeolite powder was calcined at 550°C for 4 hrs. in a muffle furnace exposed to air to convert the zeolite from the ammonium form to the protonated form (H-ZSM-5). A conventional incipient wetness impregnation method was used to prepare three different catalysts. Each catalyst was loaded with a particular weight percent metal loading: 2% Ga/H-ZSM-5 (Fresh-Ga), 1.5% Ga0.5%Pt/H-ZSM-5 (Fresh-GaPt), and 0.5%Pt/H-ZSM-5 (Fresh-Pt) catalysts. For the 2 wt. % Ga catalyst, the corresponding amount of the gallium nitrate hydrate salt was dissolved in deionized water, then added dropwise to H-ZSM-5 powder and thoroughly mixed. The catalyst was then dried in an oven at 100°C for 12 hrs. Finally, the powder was calcined in air at 550°C for 4 hrs. The Pt catalyst was prepared similarly to the Ga catalyst, whereas the bimetallic catalyst, GaPt, was made by co-impregnation method. Ga and Pt precursor solutions were made by adding the amount of each precursor, according to the desired weight percent loading, to deionized water. The two solutions of Ga and Pt precursors were then added dropwise to HZSM-5 powder simultaneously. The GaPt catalyst was then dried and calcined following the same process as the monometallic Ga and Pt catalysts. Each fresh catalyst powder was pressed and sieved between 70 and 100 mesh particle size for fixed-bed reactions.

2.2. Experimental Procedures

Prior to the ethane DHA fixed bed reaction each fresh metal promoted catalyst was pretreated by a hydrogen reduction in a conventional horizontal clam-shell furnace under continuous flow in a quartz tube. Once the fresh catalysts were pelletized, 3.0 grams of each catalyst was placed in a quartz tube using quartz wool. Each catalyst was then exposed to 100 mL/min of pure hydrogen as the reactor ramped to a temperature of 650°C at 10°C/min and then

held for 30 minutes. Following the reduction, the reduced Ga (Red-Ga), GaPt (Red-GaPt), and Pt (Red-Pt) catalysts were collected, characterized, and used in the ethane DHA reaction.

The ethane DHA reaction for each catalyst was carried out in a Micromeritics AutoChem 2950 analyzer in-line with a micro gas chromatograph (micro-GC) for gas product analysis. Within the micromeritics analyzer the lines and internal valves were heated at 150°C. At the exit of the micromeritics the tube to the micro-GC was heat traced and held at a temperature of 150 - 170°C. These heated lines allowed for the product stream to remain in the gas phase and avoid product condensation. For each experiment 300 mg of the pelletized fresh or reduced catalyst was loaded into the u-shaped quartz tube using quartz wool and then placed into the reactor. The catalyst was then heated to 615°C under inert nitrogen flow at 30 mL/min at 10°C/min. Once at reaction temperature, pure ethane was then mixed with nitrogen to make a 30% ethane mixture, with a gas hour space velocity of 6,000 mL/hr/gram catalyst, which flowed over the catalyst at 30 mL/min for 2 hrs time on stream. Following the reaction and data collection the catalysts were cooled to room temperature under 30 mL/min inert nitrogen flow and saved for further characterization.

All reactant gases were purchased from AirGas with ultrahigh-purity (UHP) grade. The product stream was analyzed by a four-channel Agilent 3000A micro-gas chromatograph (GC) following the reactor. The micro-GC contained four columns, a molecular sieve, PLOT U, aluminum, and OV-1, allowing for the analysis of hydrogen, nitrogen, methane, ethane, ethylene, propane, propylene, benzene, and toluene. The ethane conversion, product flow rate, product selectivity, and product production rate for each catalyst was calculated by the defined equations (1), (2), (3), and (4), respectively.

$$(1) \text{ Ethane Conversion (\%)} = \frac{\text{ethane fed (scm)} - \left[\frac{\text{ethane (mol\%)} \cdot \text{inert fed (scm)}}{100} \cdot \frac{\text{inert (mol\%/100)}}{\text{inert (mol\%/100)}} \right]}{\text{ethane fed (scm)}} * 100$$

$$(2) \text{ Product Flowrate (mol/min)} = \frac{\text{product (mol\%)}}{100} * \frac{\text{inert fed (scm)}}{\frac{\text{inert (mol\%)}}{100}} * [1000 * 0.08206 * (25 + 273)]$$

$$(3) \text{ Product Selectivity (\%)} = \frac{\text{product (mol\%)} * \text{product carbon \#}}{[\text{componet fed (mol\%)} - \text{componet out (mol \%)}] * \text{componet carbon \#}} * 100$$

$$(4) \text{ Production Rate } \left(\frac{\text{g}_{\text{Product}}}{\text{kg}_{\text{catalyst}} * \text{hour}} \right) = \frac{\text{product flow rate } \left(\frac{\text{mol}}{\text{min}} \right) * \text{product molecular weight } \left(\frac{\text{g}}{\text{mol}} \right) * 60 \frac{\text{min}}{\text{hour}}}{\text{kilograms}_{\text{catalyst}}}$$

2.3. Catalyst Characterization and Product Analysis

Powder X-ray Diffraction (XRD) analysis was performed on the fresh and reduced powdered samples using a PANalytical X'Pert Pro X-ray Diffractometer (XRD) working under 45 kV and 40 mA using CuK α radiation source. The scanning angle ranged from 5° to 50° (2 θ). Data analysis was completed using the Highscore Plus Analyses software supplied by PANalytical.

Inductively Coupled Plasma-Optical Emission Spectrometer (ICP-OES) was used to confirm the elemental composition of the as-prepared fresh catalyst. The samples were prepared by a sodium peroxide fusion followed by an acid digestion. Following the calcination of the fresh catalyst, 0.1g of each sample was fused with sodium peroxide. The fuseate was then dissolved in a dilute nitric acid/hydrochloric acid solution. The samples elemental analysis was performed in an Agilent 720 ICP-OES. The chemical compositions of the three different fresh catalysts are shown in Table 1.

Catalyst	Ga wt. %	Pt wt. %	SiO ₂ /Al ₂ O ₃ Ratio (SAR)
Fresh-Ga	1.8	-	24
Fresh-GaPt	1.4	0.4	25
Fresh-Pt	-	0.4	24

A JEOL-2100 High-Resolution Transmission Electron Microscope (HR-TEM) coupled with an Oxford Energy-Dispersive X-ray (EDX) was used to analyze each catalysts structural morphology. EDX was incorporated for the elemental analysis of the images. The operating voltage of the TEM was 200 kV. A small amount of each catalyst was sonicated in acetone to form a uniform cloudy solution. The TEM sample grids were prepared by evaporating a drop of the catalyst solution on to the grid. The 200 mesh formvar coated copper grids were purchased from Ted Pella, INC.

Surface area and micropore measurements were carried out on the fresh catalyst using a Micromeritics ASAP 2020+. The specific surface area was calculated using the Brunauer-Emmett-Teller (BET) model. Each sample was degassed for 6 hrs at 300°C under vacuum to remove any surface moisture and adsorbed gases. Following the degas each sample was subjected to a program consisting of the adsorption and desorption of nitrogen typically ran at -196°C.

A Temperature Programed Reduction (H₂-TPR) was performed on the fresh catalyst using a Micromeritics AutoChem 2950 equipped with a thermal conductivity detector (TCD). The samples were heated to 150°C at 10°C/min for 60 minutes under inert helium flow to remove moisture. The catalyst was then cooled to 100°C. The catalyst was then exposed to 25 mL/min of 10% hydrogen in argon for 20 minutes to acquire a baseline. Following the 20-minute hold, the catalyst was heated to 900°C at 10°C/min as the TCD signal was collected.

A Physical Electronic PHI 5000 VersaProbe X-ray Photoelectron Spectroscopy (XPS/UPS) was used to determine chemical state of the metal promoters on each fresh and reduced catalyst. The XPS was equipped with a monochromatic Al X-ray beam (100 μm, 12.5 W, 15 kV). All samples were sputtered with an Argon ion gun prior to analysis to remove surface contaminates. For each catalyst, a survey and detailed scan was obtained. The binding energies were corrected for charging effect by referring to C1s line 284.8 eV.

A Thermogravimetric Analysis (TGA) was carried out using TA Instruments SDT-650 Simultaneous Thermal Analyzer. The carbon content of the spent catalysts was determined by the HiRes Dynamic analysis mode set to a resolution number of 4 and a sensitivity value of 1, with a max heating rate of 20°C/min to 900°C in air. TA Instruments TRIOS analysis software was used to generate the TGA weight loss curves and the differential thermal analysis (DTA) curves for each catalyst.

Pyridine Diffuse Reflectance Infrared Fourier Transform Spectroscopy (Py-DRIFTS) was performed on a Thermo Scientific Nicolet iS50 FT-IR to investigate the surface acidity of the fresh and reduced catalysts. The FT-IR was fitted with a Harrick Praying Mantis Cell containing an environmental chamber, the Harrick High Temperature Vacuum Chamber (HVC), with one SiO₂ and two ZnSe transmission windows. All spectra were acquired at a 200 scans per spectrum, a 4 cm⁻¹ resolution, and in the region ranging from 650 – 4000 cm⁻¹ using a liquid-nitrogen cooled mercury-cadmium-telluride (MCT/A) detector. Each sample was degassed for 6

hrs. at 300°C prior to being loaded into the HVC chamber to remove the impurities which could possibly be adsorbed on the catalyst surface. Using a Harrick temperature controller (ATK-024-3) equipped with a Watlow EZ-Zone Configurator and a heated water bath the temperature of the DRIFTS cell was controlled. Once the powder catalyst was loaded (20 mg) into the HVC cell, the catalyst was held at 25°C and under 10 mL/min nitrogen flow. The catalyst was then heated to 150°C, 250°C, 350°C, and 450°C, respectively, and for each temperature the corresponding background spectrum was taken. The catalyst was then cooled to 25°C, where 10 mL/min of nitrogen flow was passed through a liquid feedstock of pyridine in a bubbler to dose the catalyst for one hour. After the catalyst was dosed the gas flow was switched to bypass the bubbler and used as a purge gas. The dosed sample was then held for 30 minutes before collecting sample DRIFTS spectrum under absorbance mode. The step was repeated at 150°C, 250°C, 350°C, and 450°C, respectively.

3. Results and Discussion

3.1 Characterization of Fresh and Reduced Catalysts Prior to Ethane DHA Reaction

A summary of the surface area and micropore analysis of the as-prepared fresh catalyst is shown in Table 2. All samples tested displayed a type II isotherm plot. The surface area was then analyzed and calculated using the Brunauer-Emmett-Teller (BET) model. The addition of the transition metals to the unpromoted HZSM-5 resulted in a decrease in the total BET surface area, micropore, and external surface area of the fresh catalysts. As the total weight percent of the metal loading was increased, the total BET surface area of the catalysts decreased. The addition of the Pt to the Ga catalyst resulted in a decrease in the total BET surface area and micropore surface area of the Fresh-GaPt catalyst, with no change in the external surface area.

Catalyst	BET Surface Area (m²/g)	t – plot Micropore Area (m²/g)	t – plot External Surface Area (m²/g)
H-ZSM-5	346.1086	246.9742	99.1347
Fresh - Ga	323.1480	230.9233	92.2247
Fresh - GaPt	319.0673	226.5209	92.5463
Fresh - Pt	336.1449	238.4973	97.6476

The fresh and reduced catalysts properties were analyzed using x-ray diffraction (XRD). The XRD pattern shown in Figure 1a indicated that the reduction had no effect on the crystallinity of the zeolite support, with no observable change in the characteristic peaks unique to the MFI framework observed at the diffraction angles $2\theta = 8-9^\circ$ and $22-25^\circ$.³⁹ No bulk Ga₂O₃ crystalline diffraction peaks were observed due to the low metal loading and/or the homogeneous dispersion of the Ga species on the surface of the zeolite. However, the Fresh-GaPt exhibited an additional peak at $2\theta = 39.8^\circ$ which corresponds with the metallic Pt (111) species on the surface catalyst, seen in Figure 1b.³⁹ With the reduction of the Fresh-GaPt, the Red-GaPt lost the Pt (111) peak and gained a new peak at $2\theta = 41.1^\circ$ associated with the GaPt alloy, Ga_{5.4}Pt_{10.6} phase. Lapidus et. al. showed following a hydrogen reduction at 500°C, their Pt/GaZSM-5 catalyst

exhibited no Pt (111) peak but rather the GaPt alloy species peak which they attributed to the $\text{Ga}_{5.4}\text{Pt}_{10.6}$ alloy phase.⁴⁰ The fresh and reduced Pt catalyst did not exhibit these peaks.

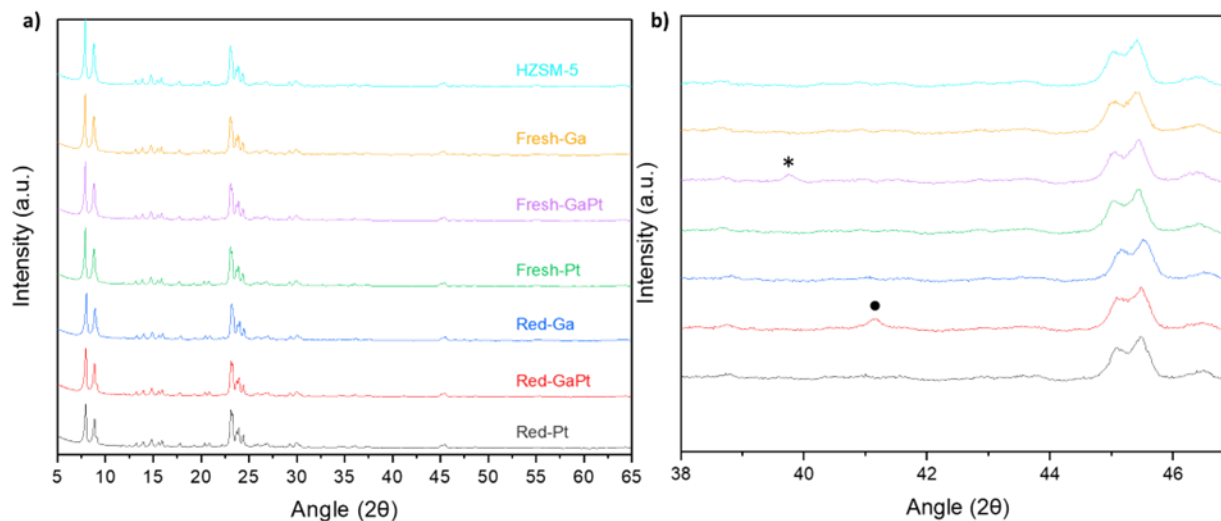


Figure 1: XRD patterns of HZSM-5, fresh, and reduced Ga, GaPt, and Pt catalyst: a) 5 - 65° and b) 38 - 47° with (*) indicating the metallic Pt species (39.8°) and (●) indicating the GaPt alloy species (41.1°).

The H_2 -TPR profiles of the fresh and reduced catalysts are displayed in Figure 2. In Figure 2a and b, the fresh catalysts, Ga and GaPt, have a small peak at 320°C which Liu et. al. attributed to the uptake of hydrogen.⁴¹ The appearance of this peak in the fresh catalysts indicates that the incipient wetness impregnation synthesis method was successful in creating a Ga_2O species, which was able to react with the Brönsted acid sites upon calcination in air to form Ga^+ . The Ga^+ species has been shown to chemisorb hydrogen at 320°C, forming a dihydro gallium complex, GaH_2^+ .⁴¹ The fresh Ga and GaPt catalyst also displayed peaks at 580°C and 520°C, respectively. The Fresh-Ga exhibited a second intense peak at 580°C which can be assigned to the reduction of Ga_2O_3 to Ga_2O .^{14, 41, 42} The addition of the Pt to the Ga catalyst resulted in a shift in the 580°C peak to the lower temperature of 520°C. This is due to the hydrogen spillover effect, which results in the acceleration of the reduction of Ga at lower temperatures.⁴³ The hydrogen spillover effect is thought to occur due to the intra-zeolitic Pt clusters ability to activate and split hydrogen over the gallium oxide particles forming Ga^+ active sites on the external surface of the zeolite framework which can form dihydro gallium complexes.⁴⁴ The effectiveness of the pretreatment reduction process of the fresh catalysts was tested by hydrogen temperature programmed reduction (H_2 -TPR) to confirm the reduction of the Ga and Pt species on the three different catalysts. Due to the pre-reduction of the catalyst at 650°C, both the Red-Ga and Red-GaPt exhibit the loss of the 580°C and 520°C peaks, respectively, and show the appearance of a lower temperature intense peak at 320°C. As stated previously, the peak at 320°C in the Red-Ga and Red-GaPt is due to the increased population of Ga^+ which can uptake hydrogen to form dihydro gallium complexes, GaH_2^+ .^{41, 45} This was confirmed by Hensen et. al. using in situ Ga K-edge XANES, proving the formation of a Ga^+ species following the hydrogen reduction of fresh Ga-HZSM-5 at a temperature above 400°C.⁴² The pretreatment reduction of the catalyst proved successful in sufficiently reducing the Ga species on the zeolite surface. In Figure 2c, the Fresh-Pt catalyst experienced two reduction peaks, one around 166°C and another around 385°C. The

low temperature peak corresponds to the reduction of Pt^{2+} to Pt^0 and weak interaction with the support. The second peak indicates a strong interaction between Pt and the surface of the support.^{14, 41, 46} Following the hydrogen reduction of the bulk Fresh-Pt the second H_2 -TPR show the catalyst was fully reduced.

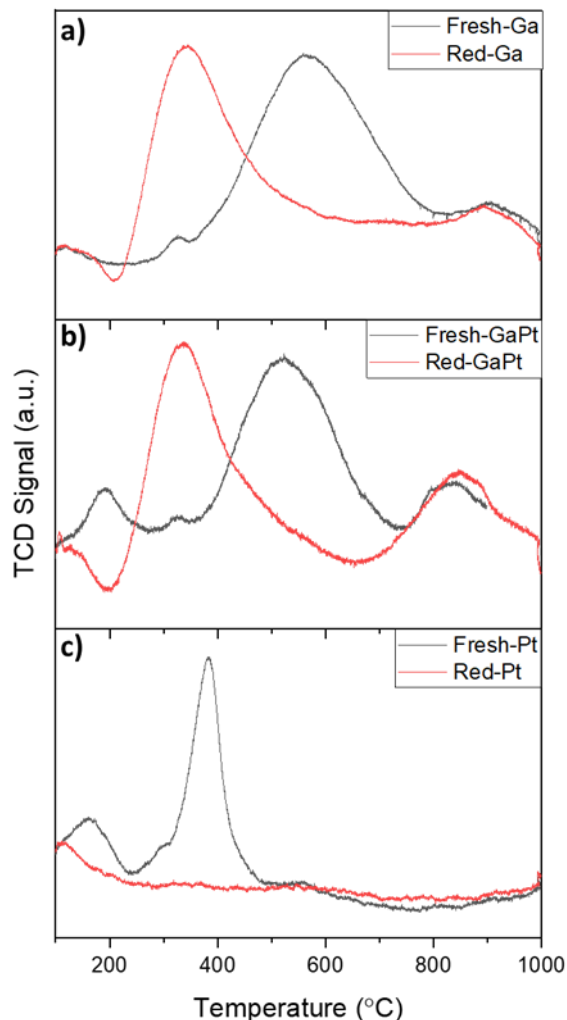


Figure 2: Hydrogen temperature programmed reduction (H_2 -TPR) of the fresh and reduced catalysts. (a) Fresh-Ga and Red-Ga, (b) Fresh-GaPt and Red-GaPt, and (c) Fresh-Pt and Red-Pt.

The surface composition and chemical oxidation states of the elemental promoters for each as-prepared fresh and reduced catalyst was analyzed using XPS. The characterization of the Ga and Pt species can provide information on the dispersion and interaction of the promoter species on the surface of the support. The peak fitted Ga $2p_{3/2}$ region can be seen in Figure 3. As seen in Figure 3, the Fresh-Ga and the Fresh-GaPt showed two peaks at 1120.0 eV and 1118.7 eV. The higher binding energy peak corresponds to the framework Ga species and/or cationic GaO^+ , and the peak at lower binding energy extra-framework Ga_2O_3 .^{14, 41, 45} A shift from the pure Ga_2O_3 binding energy of 1117.8 eV to the higher binding energy of 1118.7 eV can be observed.⁴³ Liu et. al. attributed this shift in the binding energy of the Ga $2p_{3/2}$ region, specifically the Ga_2O_3 peak, to the dispersion of the Ga species on the surface of the catalyst.⁴¹ The XPS

spectra for the reduced catalyst in the Ga $2p_{3/2}$ region show a loss of peak intensity indicating the high dispersion of the metal species on the zeolite surface. For the Red-Ga and Red-GaPt catalysts, the intensity loss indicates the penetration of the Ga species into the zeolite pores and ion exchange of the metal promoters with the Brönsted acid sites.^{14, 38, 41-43} The Red-Ga and Red-GaPt catalyst XPS exhibited a shift in speciation to the higher binding energy to 1120.0 eV. The shift to the higher binding energy when compared to the fresh catalysts, indicates the increased presence of the Ga⁺ and/or GaO⁺ on the external surface following the reduction of the catalyst.

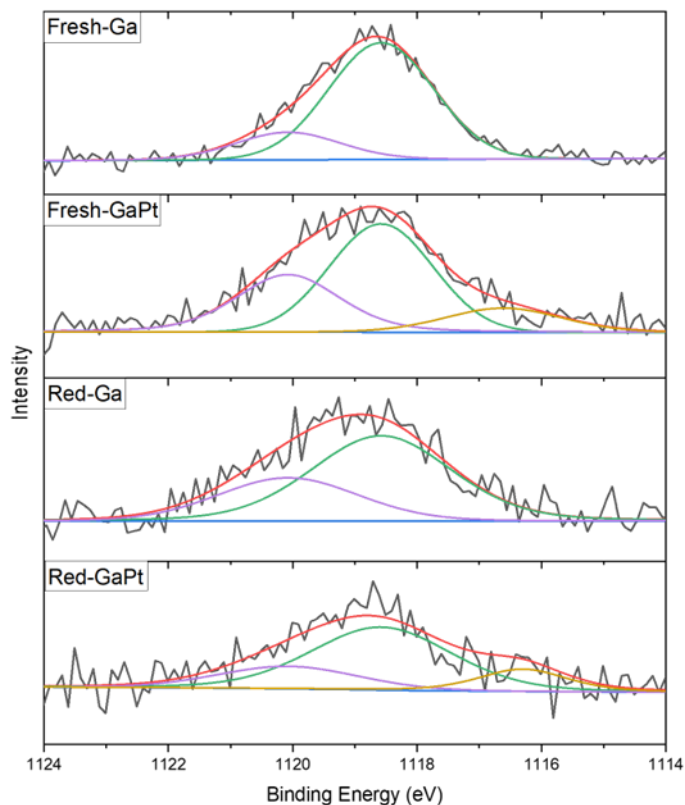


Figure 3: XPS of the fresh and reduced gallium containing catalysts, Fresh-Ga, Fresh-GaPt, Red-Ga, and Red-GaPt in the Ga $2p_{3/2}$ region.

The Al $2p$ peak and the Pt $4f$ peaks experience a very strong overlap in the 68-82 eV range, which could partially be resolved with the detailed scan and peak fitting, shown in Figure 4. The shoulder at 71 eV of the Al $2p$ peak around 75 eV indicates the existence of the Pt $4f$ peaks for all the platinum containing catalysts. This shoulder was not present in the fresh-Ga or red-Ga catalysts. The fresh GaPt and Pt when fitted, resolved both the Pt $4f_{7/2}$ and the Pt $4f_{5/2}$ peaks at 71 eV and 75 eV, respectively. Duan et al. associated the peaks at 71 eV and 75 eV with the Pt⁰ and Pt²⁺, respectively. In the reduced GaPt and Pt catalyst, the Pt $4f_{5/2}$ could not be resolved which confirms the reduction of the Pt²⁺, which is consistent with the H₂-TPR.^{41, 46}

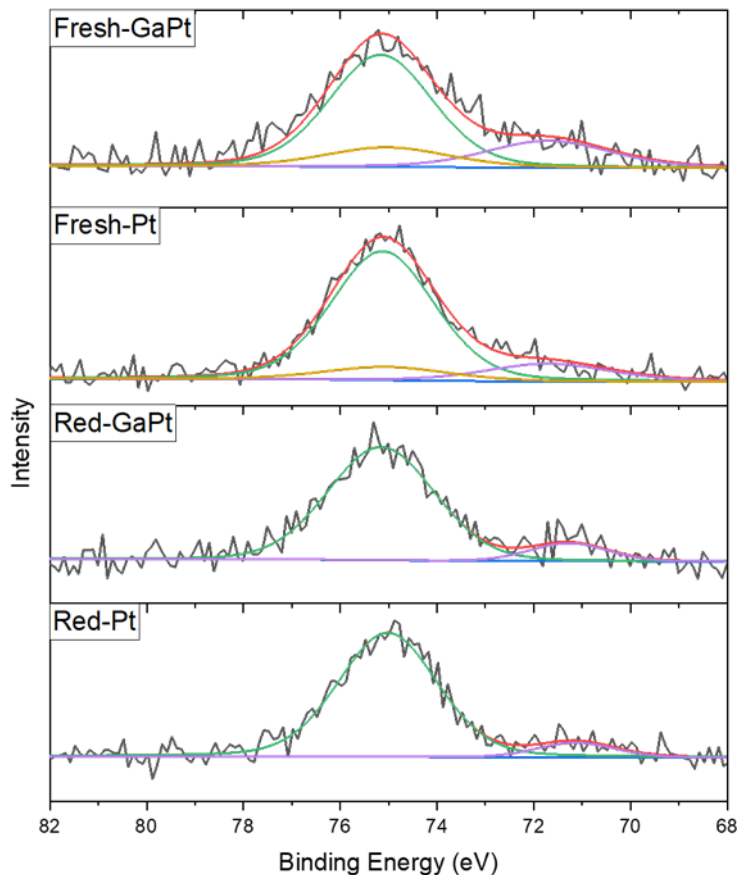


Figure 4: XPS of the fresh and reduced platinum containing catalysts in the Al 2p, Pt 4f region.

3.2 Investigation of the Acidity of Fresh and Reduced Catalysts Prior to Ethane DHA Reaction by Pyridine FT-IR DRIFTS

Pyridine FT-IR DRIFTS was utilized to elucidate the acidic properties of the fresh and reduced catalysts. The interaction of the metal promoters with the zeolite's different acid sites and their distribution was investigated. The H-ZSM-5 support contains a bridging hydroxyl groups (Al-OH⁺-Si) which are known as the Brönsted acid sites. The Brönsted acid sites are a proton donor, which can protonate the dosed pyridine to form pyridinium ions. These ions display a distinct C-C stretching vibrational frequency at 1550 cm⁻¹. The Lewis acid sites are associated with the extra-framework Al-containing species. Typically, the Lewis acid sites shows a band around 1450 cm⁻¹. The additional peak at 1490 cm⁻¹ represents a combination of the two acid sites.^{25, 32, 35, 36}

The 350°C spectra for each catalyst between 1425-1575 cm⁻¹ is seen in Figure 5. At 350°C and higher the physisorbed pyridine was determined to be completely removed, leaving only the chemisorbed pyridine, thus giving the Brönsted/Lewis (B/L) acid site ratios for the fresh and reduced catalyst, seen in Table 3. The ratio of each catalysts Brönsted to Lewis acid sites was determined by the peak areas of the unique adsorption bands at each purge temperature. Looking at 350°C, all metal loaded catalysts showed a decrease in their B/L acid site ratio when

compared to the fresh H-ZSM-5, indicating that the metal promoters interact with the zeolite's surface affecting the acidity of the catalyst. The monometallic Ga catalyst experiences a decrease in B/L ratio following the hydrogen reduction of the fresh catalyst, from the Fresh-Ga to the Red-Ga. The Ga species is known to replace the proton associated with the zeolites Brönsted acid sites.^{18, 20} As seen in the H₂-TPR the Fresh-Ga observed little uptake of hydrogen indicating there was low concentrations of the Ga₂O or cationic Ga⁺ species prior to the reduction. Following the reduction, the increased presence of the reduced Ga species would result in a decrease in the Brönsted acid sites and an increase in Lewis acid sites.^{35, 41} Both GaPt and Pt exhibited a small increase in B/L ratio following the reduction of the fresh catalysts. The formation of the GaPt alloy in the Red-GaPt could potentially be affecting the ability of the Ga species to exchange with the Brönsted acid sites of the catalyst, therefore leading to the increase in the B/L acid site ratio. The Pt species has little to no effect on the Brönsted acid sites but has been known to increase the Lewis acidity of the catalyst.²⁰

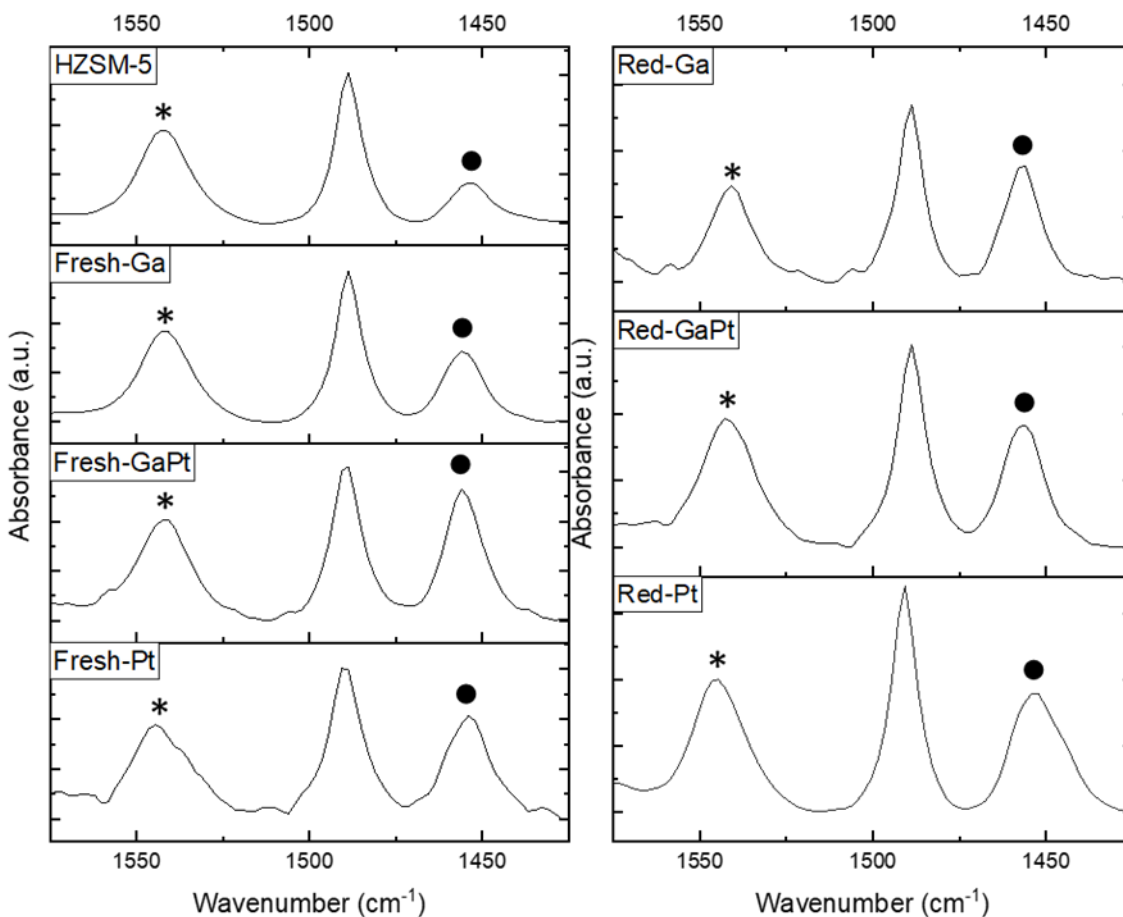


Figure 5: FT-IR pyridine DRIFTS spectra for both fresh and reduced catalyst at 350°C. The Brönsted acid sites (*) are seen around 1550 cm⁻¹ and the Lewis acid sites (●) around 1450 cm⁻¹.

Table 3: Brönsted/Lewis Acid Site Ratio Acquired from FT-IR Pyridine DRIFTS	
Catalyst	Brönsted/Lewis Acid Site Ratio at 350°C
HZSM-5	2.53
Fresh-Ga	1.69
Fresh-GaPt	0.96
Fresh-Pt	0.86
Red-Ga	1.11
Red-GaPt	1.24
Red-Pt	0.99

3.3 The Performance of the Catalyst in Ethane Dehydroaromatization

The catalytic performance of HZSM-5, the three as-prepared fresh and the three reduced Ga, GaPt, and Pt catalysts were acquired during the dehydroaromatization of ethane at 615°C for over 2-hrs time on stream. The ethane conversion and product selectivity for each catalyst is shown in Figures 6 & 7, respectively. As seen in Figure 6, the support, HZSM-5, has little to no conversion over the course of the 2-hr reaction, indicating the addition of the metal promoters are the primary source of reactivity. The addition of Ga to the HZSM-5 support resulted in an increase in conversion from 4.5% to 22.8% for Fresh-Ga and 24.2% for Red-Ga at 21 minutes time-on-stream (TOS). The reduction of the Fresh-Ga produced a small increase in conversion in the Red-Ga catalyst, which is consistent with Liu et. al. findings for the dehydroaromatization of propane over GaZSM-5.⁴¹ The product selectivity's of the Fresh-Ga and Red-Ga catalyst exhibited a similar trend, seen in Figure 7. However, the Fresh-Ga exhibited a higher selectivity toward methane and a lower selectivity towards ethylene initially, indicating that the Fresh-Ga undergoes a reduction to form the Ga⁺ active species. It is important to note that an oxidation treatment following the reduction of the fresh Ga catalyst has shown to increase conversion and product selectivity to desired products. With the oxidation of the Ga⁺ and GaH₂⁺ species an increased population of the active GaO⁺ species would occur.^{41, 47}

The Fresh-Pt catalyst exhibited an increase in conversion following the reduction from 35.7% to 43.8% in the Red-Pt catalyst. The Pt catalysts experienced a faster deactivation than the Ga or GaPt catalysts. The Fresh-Pt and Red-Pt catalyst exhibited a similar product selectivity for the first 60 minutes TOS. The reduction of the Fresh-Pt catalyst improved the stability of the conversion and product selectivity of the Red-Pt catalyst. After 60 minutes TOS the Red-Pt exhibited an increasing selectivity towards C3 hydrocarbons, which is due to the higher dispersion of the Pt species on the zeolite.²³ The increased selectivity leads to an increase in the coke deposition rate. The product selectivity of the Fresh-Pt catalyst suggests the fresh catalyst favors the cleavage of C-C bonds due to the higher methane and ethylene selectivity and lower C3 hydrocarbon selectivity.

The addition of Pt to the Fresh-Ga catalyst, Fresh-GaPt, produced an increase in conversion of 22.8% to 53.8%. An additional increase in conversion was observed following the reduction of the fresh catalyst to the Red-GaPt catalyst, which has a conversion of 58.2% at 21 minutes TOS. As previously discussed, the addition of Pt to the Ga/ZSM-5 catalyst results in the increased reducibility of the gallium species through the hydrogen spillover effect.^{14, 18, 43} The addition of Pt to Ga/ZSM-5 under H₂-pretreatments has been shown to lead to the formation of Ga_{5.4}Pt_{10.6} alloy particles, as seen in Figure 1b.⁴⁸ The formation of the GaPt alloy has been

attributed to the long-term stability of the conversion and product selectivity. The Fresh-GaPt catalyst exhibited a lower initial methane and benzene selectivity in comparison to that of the Red-GaPt. This suggests that the fresh catalyst undergoes an induction period where the Ga and Pt species became fully reduced and the Pt-Ga alloy formed.^{17, 18, 22, 49, 50}

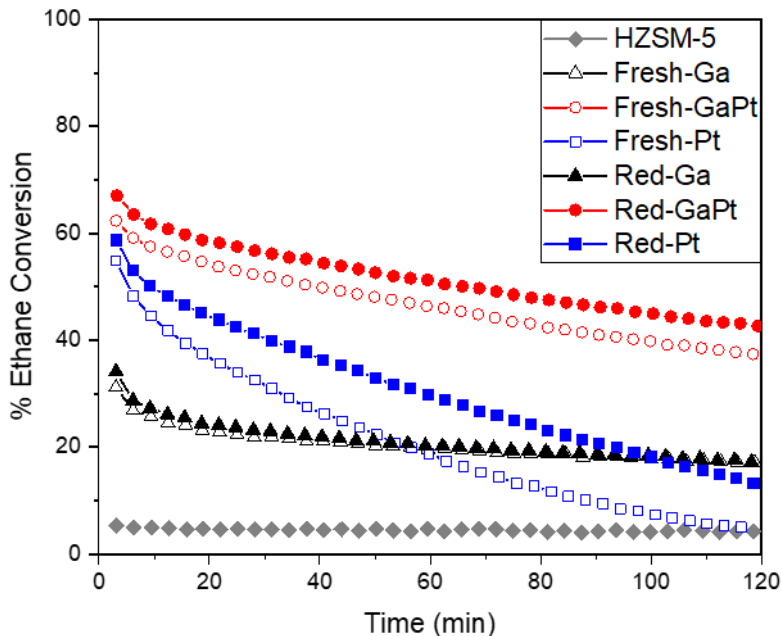


Figure 6: Ethane conversion (%) for unpromoted HZSM-5 support, the three fresh catalysts, and the three reduced Ga, GaPt, and Pt catalysts over the 2-hrs reaction period at 615°C.

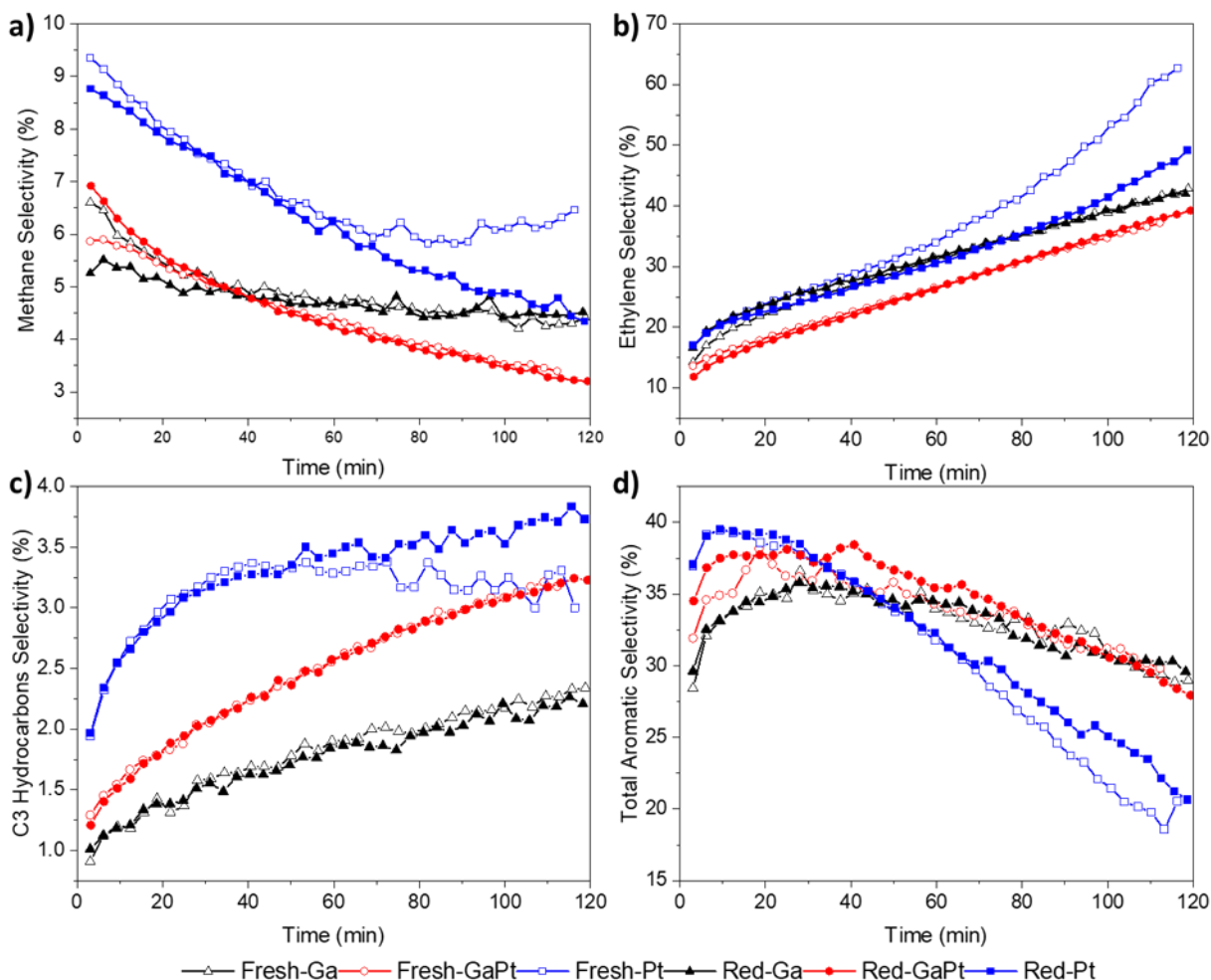


Figure 7: Comparison of the product selectivity for the fresh and reduced Ga, GaPt, and Pt catalyst in a conventional fixed bed at 615°C for 2-hrs; (a) methane selectivity, (b) ethylene selectivity, (c) C3 hydrocarbon selectivity, and (d) total aromatic selectivity.

3.2 Characterization of Fresh and Reduced Catalysts Following the Ethane DHA Reaction

A thermogravimetric analysis (TGA) and differential thermal analysis (DTA) was performed on the spent fresh and reduced catalysts to investigate the coke deposited on the catalyst surface during the 2 hrs TOS, seen in Figure 8. Each catalyst was exposed to an oxidative environment to determine the potential coke formations which accumulated on the surface of the catalysts. Literature has indicated that cracking of ethylene inside the zeolite channel can lead to soft coke or low temperature burn-off coke. Whereas hard coke or high temperature burn-off coke is attributed to the polycondensation of aromatics on the external surface of the zeolite and/or at the Brönsted acid sites.^{18, 49} As seen in the DTA curves, the positive peaks indicate each catalyst goes through a highly exothermic process due to coke burn-off and/or oxidation of the metal species on the catalyst.⁵² In the TGA profile in Figure 6, the fresh and reduced Ga promoted catalysts both experience a single weight loss at 600°C, which suggests the presence of a single type of hard coke carbon species. The single weight loss at

600°C for Ga catalysts has been attributed to the combustion of coke within the zeolite pores.⁵³ The fresh and reduced Ga catalyst experiences a 3.8% and 3.6% weight loss, respectively. The fresh and reduced Pt catalysts both exhibit two weight loss peaks at 520°C and 600°C, which were attributed to soft and hard coke, respectively. The overall weight loss of the Fresh-Pt and the Red-Pt was 4.1% and 6.0%, respectively. The Red-Pt species exhibited a higher weight loss, which is consistent with the reaction data, showing the increased stability toward C3 hydrocarbon selectivity.²³ The fresh and reduced GaPt catalysts both exhibit three weight loss peaks at 535°C, 575°C, and 625°C, indicating the presence of soft and hard coke. Samanta et. al. observed a hard coke, polyaromatic coke, species over their Ga and Pt containing catalysts.¹⁸ The overall weight loss of the Fresh-GaPt and the Red-GaPt was 6.1% and 6.2%, respectively.

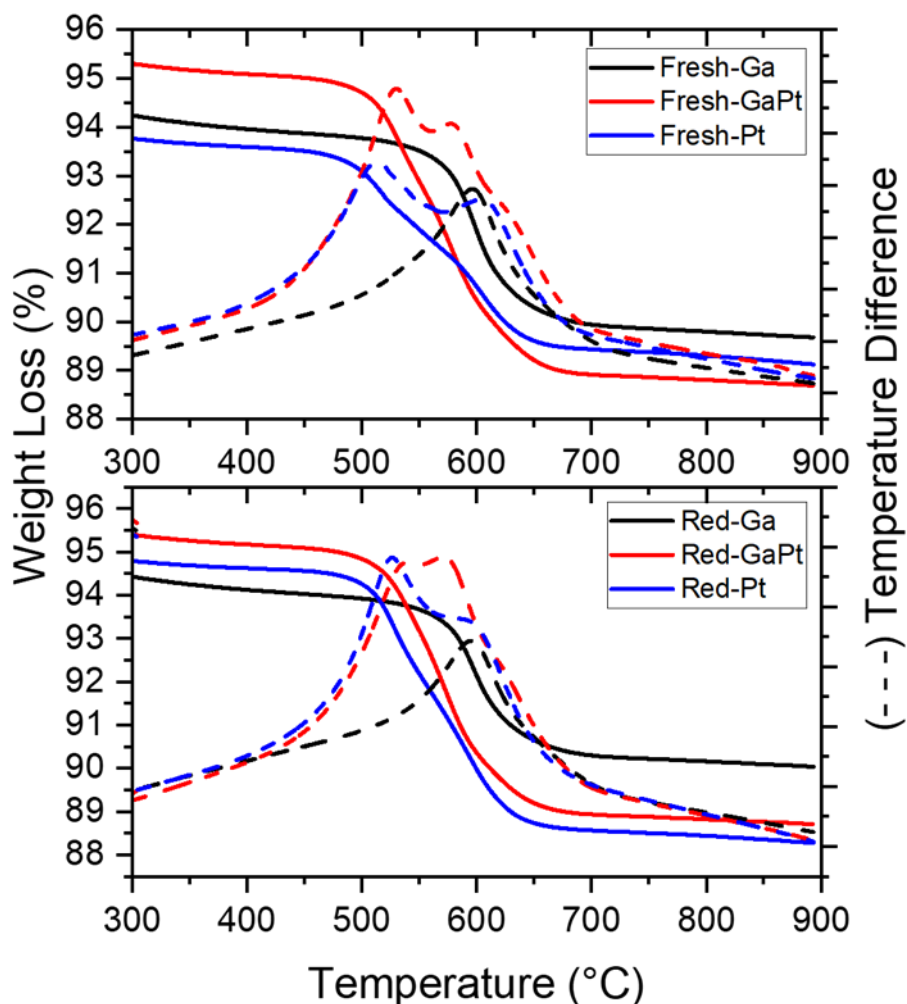


Figure 8: Thermogravimetric analysis (TGA) and differential thermal analysis (DTA) of the spent fresh and reduced catalysts after the 2-hour reaction.

Since the GaPt showed the best catalytic performance an investigation of possible metal agglomeration and deactivation of the fresh and reduced GaPt catalyst was carried out using a TEM/EDX. In Figure 9a, the Fresh-GaPt showed to have well dispersed metal particles on the surface of the support. Bai et al. illustrated that the synthesis of the GaPt catalyst via incipient

wetness impregnation can produce well dispersed metal particles on the surface of the fresh catalyst without reduction.¹⁷ Following the ethane dehydroaromatization reaction of the Fresh-GaPt catalyst, in Figure 9b, a metal agglomerate around 50 nm in size was observed in the spent catalyst's TEM image. After the reduction of the catalyst, the Red-GaPt catalyst still exhibited well dispersed particles, seen in Figure 9c, indicating the reduction did not cause any metal agglomeration on the catalyst surface. The spent Red-GaPt catalyst shows partial migration of the metals on the surface, forming a metal agglomerate around 20 nm in size, seen in Figure 9d. This suggests that the reduction of the catalyst can help partially maintain well dispersed metal particles with the formation small agglomerate following a reaction compared to the fresh.

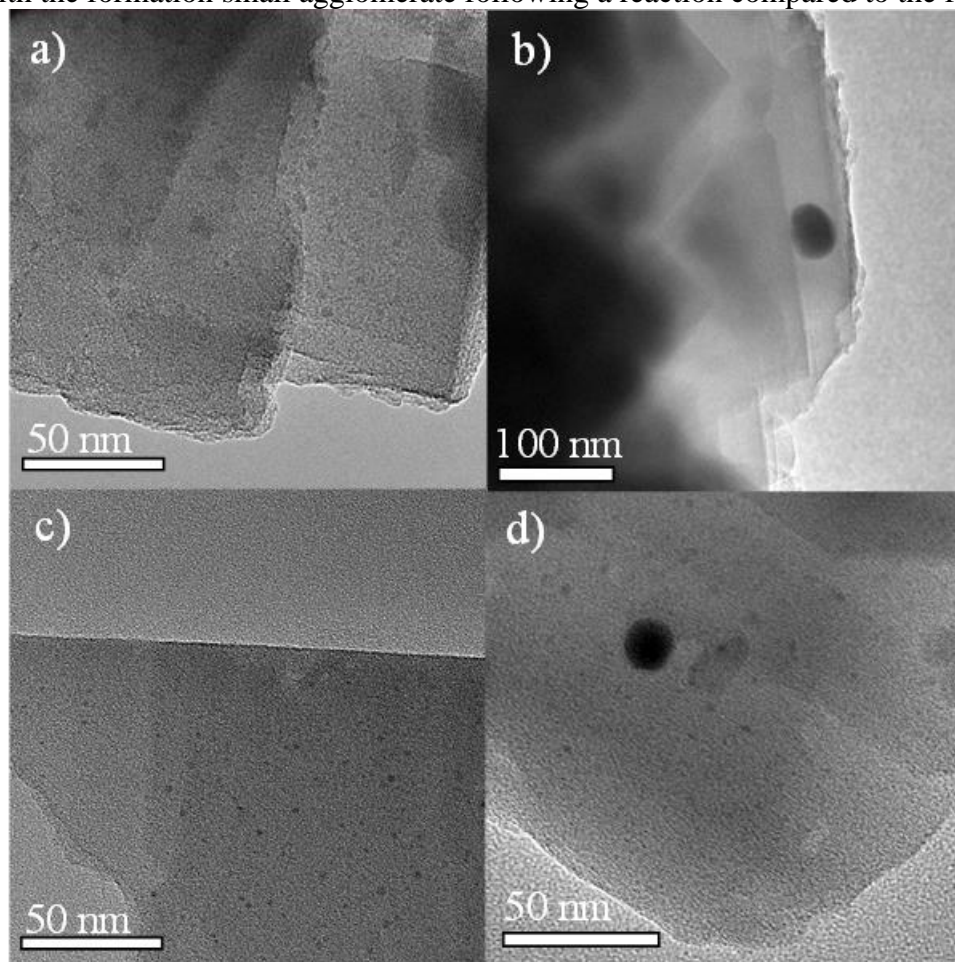


Figure 9: TEM images of fresh and reduced GaPt catalyst before and after the ethane DHA reaction: (a) Fresh-GaPt, (b) Spent Fresh-GaPt, (c) Red-GaPt, and (d) Spent Red-GaPt.

4. Conclusion

The ethane dehydroaromatization reaction was studied over HZSM-5, fresh and reduced zeolite-supported Ga, GaPt, and Pt catalysts to assess their catalytic performance. The effectiveness of the hydrogen reduction of each fresh catalyst was confirmed by H₂-TPR. The fresh Ga and GaPt catalyst experienced the reduction of the Ga₂O₃ species to a Ga₂O, which can then interact with the Brønsted acid site proton forming Ga⁺ species on the surface. The addition of the Pt to the Ga catalyst accelerated the reduction of the Ga species by the hydrogen spillover

mechanism. The Pt catalysts showed a full reduction in the H₂-TPR curve. The shift in the Ga2p_{3/2} region for all Ga containing catalysts, from the lower binding energy pure Ga₂O₃, indicated the well dispersion of the Ga species on the surface of the zeolite in both the Ga and GaPt catalysts. The XRD indicated that following the hydrogen reduction of the GaPt catalyst, there was a loss of the metallic Pt peak was observed and there was a formation of a GaPt alloy species peak. The reduction of the GaPt catalyst shows to be vital in the increased ethane conversion but shows little change in product selectivity. The Pt and Ga species synergistically promote the ethane dehydroaromatization in the fresh and reduced GaPt catalyst.

Acknowledgements

The authors acknowledge financial support from West Virginia Higher Education Policy Commission under the grant number HEPC.drs.18.7. The authors also acknowledge financial support from AIChE RAPID Manufacturing Institute under the contract #DEEE0007888-6.7.

References

- (1) Slav, I. Natural gas demand will grow for decades to come
<https://oilprice.com/Energy/Natural-Gas/Natural-Gas-Demand-Will-Grow-For-Decades-To-Come.html>.
- (2) Venkataramen, V. K.; Guthrie, H. D.; Avellanet, R. A.; Driscoll, D. J. Program and Commercialization Strategy FETC Gas to Liquids Program. **1998**, *119* (3), 913–918.
- (3) Holmen, A. Direct Conversion of Methane to Fuels and Chemicals. *Catal. Today* **2009**, *142* (1–2), 2–8.
- (4) Spivey, J. J.; Hutchings, G. Catalytic Aromatization of Methane. *Chem. Soc. Rev.* **2014**, *43* (3), 792–803.
- (5) Horn, R.; Schlögl, R. Methane Activation by Heterogeneous Catalysis. *Catal. Letters* **2015**, *145* (1), 23–39.
- (6) Hagen, A.; Roessner, F. Ethane to Aromatic Hydrocarbons: Past, Present, Future. *Catal. Rev. - Sci. Eng.* **2000**, *42* (4), 403–437.
- (7) Lunsford, J. H. Catalytic Conversion of Methane to More Useful Chemicals and Fuels: A Challenge for the 21st Century. *Catal. Today* **2000**, *63* (2–4), 165–174.
- (8) Skutil, K.; Taniewski, M. Some Technological Aspects of Methane Aromatization (Direct and via Oxidative Coupling). *Fuel Process. Technol.* **2006**, *87* (6), 511–521.

- (9) Argyle, M. D.; Bartholomew, C. H. Heterogeneous Catalyst Deactivation and Regeneration: A Review. *Catalysts* **2015**, *5* (1), 145–269.
- (10) Saito, H.; Sekine, Y. Catalytic Conversion of Ethane to Valuable Products through Non-Oxidative Dehydrogenation and Dehydroaromatization. *RSC Adv.* **2020**, *10* (36), 21427–21453.
- (11) Xiang, Y.; Wang, H.; Cheng, J.; Matsubu, J. Progress and Prospects in Catalytic Ethane Aromatization. *Catal. Sci. Technol.* **2018**, *8* (6), 1500–1516.
- (12) Tshabalala, T. E.; Coville, N. J.; Scurrall, M. S. Dehydroaromatization of Methane over Doped Pt/Mo/H-ZSM-5 Zeolite Catalysts: The Promotional Effect of Tin. *Appl. Catal. A Gen.* **2014**, *485*, 238–244.
- (13) Robinson, B.; Bai, X.; Samanta, A.; Abdelsayed, V.; Shekhawat, D.; Hu, J. Stability of Fe- and Zn-Promoted Mo/ZSM-5 Catalysts for Ethane Dehydroaromatization in Cyclic Operation Mode. *Energy and Fuels* **2018**, *32* (7), 7810–7819.
- (14) Wang, Y.; Caiola, A.; Robinson, B.; Li, Q.; Hu, J. Hierarchical Galloaluminosilicate MFI Catalysts for Ethane Nonoxidative Dehydroaromatization. *Energy & Fuels* **2020**, *34* (3), 3100–3109.
- (15) Terunuma, R.; Saito, H.; Yabe, T.; Ogo, S. Ethane Dehydroaromatization over Co / H-ZSM-5 Catalyst. 3–4.
- (16) Ma, L.; Zou, X. Cooperative Catalysis of Metal and Acid Functions in Re-HZSM-5 Catalysts for Ethane Dehydroaromatization. *Appl. Catal. B Environ.* **2019**, *243*, 703–710.
- (17) Bai, X.; Samanta, A.; Robinson, B.; Li, L.; Hu, J. Deactivation Mechanism and Regeneration Study of Ga-Pt Promoted HZSM-5 Catalyst in Ethane Dehydroaromatization. *Ind. Eng. Chem. Res.* **2018**, *57* (13), 4505–4513.
- (18) Samanta, A.; Bai, X.; Robinson, B.; Chen, H.; Hu, J. Conversion of Light Alkane to Value-Added Chemicals over ZSM-5/Metal Promoted Catalysts. *Ind. Eng. Chem. Res.* **2017**, *56* (39), 11006–11012.
- (19) V.I. Yakerson, T.V. Vasina, L.I. Lafer, V.P. Sytnyk, G.L. Dykh, A.V. Mokhov, O. V. B. and K. M. M. The Properties of Zinc and Gallium Containing Pentasils - The Catalysts for the Aromatization of Lower Alkanes. *Sci. J C Baltzer A G Company, Publ.* **1989**, *3* (April), 8–10.
- (20) Chetina, O. V.; Vasina, T. V.; Lunin, V. V. Aromatization of Ethane over Pt,Ga/HZSM-5 Catalyst and the Effect of Intermetallic Hydrogen Acceptor on the Reaction. *Appl. Catal.*

A, Gen. **1995**, *131* (1), 7–14.

- (21) Xu, B.; Tan, M.; Wu, X.; Geng, H.; Song, F.; Ma, Q.; Luan, C.; Yang, G.; Tan, Y. Effects of Silylation on Ga/HZSM-5 for Improved Propane Dehydroaromatization. *Fuel* **2021**, *283* (July 2020), 118889.
- (22) Sattler, J. J. H. B.; Gonzalez-Jimenez, I. D.; Luo, L.; Stears, B. A.; Malek, A.; Barton, D. G.; Kilos, B. A.; Kaminsky, M. P.; Verhoeven, T. W. G. M.; Koers, E. J.; Baldus, M.; Weckhuysen, B. M. Platinum-Promoted Ga/Al₂O₃ as Highly Active, Selective, and Stable Catalyst for the Dehydrogenation of Propane. *Angew. Chemie - Int. Ed.* **2014**, *53* (35), 9251–9256.
- (23) Reschetilowski, W.; Mroczek, U.; Steinberg, K. H.; Wendlandt, K. P. Influence of Platinum Dispersion on the Ethane Aromatization on Pt/H-ZSM-5 Zeolites. *Appl. Catal.* **1991**, *78* (2), 257–264.
- (24) Kosinov, N.; Liu, C.; Hensen, E. J. M.; Pidko, E. A. Engineering of Transition Metal Catalysts Confined in Zeolites. *Chem. Mater.* **2018**, *30* (10), 3177–3198.
- (25) Al-dughaiter, A. S.; Lasa, H. De. HZSM-5 Zeolites with Different SiO₂/Al₂O₃ Ratios. Characterization and NH₃ Desorption Kinetics. *Inorg Chem* **2014**, *53* (40), 103–131.
- (26) Zoubida, L.; Hichem, B. The Nanostructure Zeolites MFI-Type ZSM5. *Nanocrystals and Nanostructures* **2018**.
- (27) Isernia, L. F. FTIR Study of the Relation, between Extra-Framework Aluminum Species and the Adsorbed Molecular Water, and Its Effect on the Acidity in ZSM-5 Steamed Zeolite. *Mater. Res.* **2013**, *16* (4), 792–802.
- (28) Bräuer, P.; Ng, P. L.; Situmorang, O.; Hitchcock, I.; D'Agostino, C. Effect of Al Content on Number and Location of Hydroxyl Acid Species in Zeolites: A DRIFTS Quantitative Protocol without the Need for Molar Extinction Coefficients. *RSC Adv.* **2017**, *7* (83), 52604–52613.
- (29) Julbe, A.; Drobek, M.; Européen, I.; De, U. Encyclopedia of Membranes. *Encycl. Membr.* **2016**.
- (30) Wang, C.; Leng, S.; Guo, H.; Yu, J.; Li, W.; Cao, L.; Huang, J. Quantitative Arrangement of Si/Al Ratio of Natural Zeolite Using Acid Treatment. *Appl. Surf. Sci.* **2019**, *498* (September), 143874.
- (31) Sarti, E.; Chenet, T.; Pasti, L.; Cavazzini, A.; Rodeghero, E.; Martucci, A. Effect of Silica Alumina Ratio and Thermal Treatment of Beta Zeolites on the Adsorption of Toluene

from Aqueous Solutions. *Minerals* **2017**, 7 (2).

- (32) Yazici, D. T.; Bilgiç, C. Determining the Surface Acidic Properties of Solid Catalysts by Amine Titration Using Hammett Indicators and FTIR-Pyridine Adsorption Methods. *Surf. Interface Anal.* **2010**, 42 (6–7), 959–962.
- (33) Platon, A.; Thomson, W. J. Quantitative Lewis/Bronsted Ratios Using DRIFTS. *Ind. Eng. Chem. Res.* **2003**, 42, 5988–5992.
- (34) Forni, L.; Magni, E. Temperature-Programmed Desorption Study of Ammonia Desorption-Diffusion in Molecular Sieves. I. Theory. *J. Catal.* **1988**, 112 (2), 437–443.
- (35) Schreiber, M. W.; Plaisance, C. P.; Baumgärtl, M.; Reuter, K.; Jentys, A.; Bermejo-Deval, R.; Lercher, J. A. Lewis-Brønsted Acid Pairs in Ga/H-ZSM-5 to Catalyze Dehydrogenation of Light Alkanes. *J. Am. Chem. Soc.* **2018**, 140 (14), 4849–4859.
- (36) He, P.; Lou, Y.; Song, H. Olefin Upgrading under Methane Environment over Ag-Ga/ZSM-5 Catalyst. *Fuel* **2016**, 182, 577–587.
- (37) Uslamin, E. A.; Saito, H.; Sekine, Y.; Hensen, E. J. M.; Kosinov, N. Different Mechanisms of Ethane Aromatization over Mo/ZSM-5 and Ga/ZSM-5 Catalysts. *Catal. Today* **2020**, 369 (October 2019), 184–192.
- (38) Zhou, Y.; Thirumalai, H.; Smith, S. K.; Whitmire, K. H.; Liu, J.; Frenkel, A. I.; Grabow, L. C.; Rimer, J. D. Ethylene Dehydroaromatization over Ga-ZSM-5 Catalysts: Nature and Role of Gallium Speciation. *Angew. Chemie - Int. Ed.* **2020**, 59 (44), 19592–19601.
- (39) Zou, S.; Zhang, M.; Mo, S.; Cheng, H.; Fu, M.; Chen, P.; Chen, L.; Shi, W.; Ye, D. Catalytic Performance of Toluene Combustion over Pt Nanoparticles Supported on Pore-Modified Macro-Meso-Microporous Zeolite Foam. *Nanomaterials* **2020**, 10 (1).
- (40) Lapidus, A. L.; Mikhailov, M. N.; Dergachev, A. A.; Zhidomirov, G. M.; Mishin, I. V. The Nature of Active Sites in Pt Promoted GaZSM-5 Catalysts. *React. Kinet. Catal. Lett.* **2006**, 87 (2), 249–254.
- (41) Liu, R. L.; Zhu, H. Q.; Wu, Z. W.; Qin, Z. F.; Fan, W. Bin; Wang, J. G. Aromatization of Propane over Ga-Modified ZSM-5 Catalysts. *Ranliao Huaxue Xuebao/Journal Fuel Chem. Technol.* **2015**, 43 (8), 961–969.
- (42) Hensen, E. J. M.; García-Sánchez, M.; Rane, N.; Magusin, P. C. M. M.; Liu, P. H.; Chao, K. J.; Van Santen, R. A. In Situ Ga K Edge XANES Study of the Activation of Ga/ZSM-5 Prepared by Chemical Vapor Deposition of Trimethylgallium. *Catal. Letters* **2005**, 101 (1–2), 79–85.

- (43) Shpiro, E. S.; Shevchenko, D. P.; Tkachenko, O. P.; Dmitriev, R. V. Platinum Promoting Effects in Pt/Ga Zeolite Catalysts of Lower Alkane Aromatization. I. Ga and Pt Electronic States, Dispersion and Distribution in Zeolite Crystals in Dependence of Preparation Techniques. Dynamic Effects Caused by Reaction Mixture. *Appl. Catal. A, Gen.* **1994**, *107* (2), 147–164.
- (44) Fricke, R.; Kosslick, H.; Lischke, G.; Richter, M. Incorporation of Gallium into Zeolites: Syntheses, Properties and Catalytic Application. *Chem. Rev.* **2000**, *100* (6), 2303–2405.
- (45) Ausavasukhi, A.; Sooknoi, T. Tunable Activity of [Ga]HZSM-5 with H₂ Treatment: Ethane Dehydrogenation. *Catal. Commun.* **2014**, *45*, 63–68.
- (46) Duan, H.; Tian, Y.; Gong, S.; Zhang, B.; Lu, Z.; Xia, Y.; Shi, Y.; Qiao, C. Effects of Crystallite Sizes of Pt/Hzsm-5 Zeolite Catalysts on the Hydrodeoxygenation of Guaiacol. *Nanomaterials* **2020**, *10* (11), 1–19.
- (47) Nowak, I.; Quartararo, J.; Derouane, E. G.; Védrine, J. C. Effect of H₂-O₂ Pre-Treatments on the State of Gallium in Ga/H-ZSM-5 Propane Aromatisation Catalysts. *Appl. Catal. A Gen.* **2003**, *251* (1), 107–120.
- (48) Lapidus, A. L.; Mikhailov, M. N.; Dergachev, A. A.; Mishin, I. V. Structure of Active Sites of Ga-Pt Zeolite Catalysts of Alkane Aromatization. *Dokl. Phys. Chem.* **2006**, *408* (2), 175–177.
- (49) Mikhailov, M. N.; Mishin, I. V.; Kustov, L. M.; Lapidus, A. L. Structure and Reactivity of Pt/GaZSM-5 Aromatization Catalyst. *Microporous Mesoporous Mater.* **2007**, *104* (1–3), 145–150.
- (50) Siddiqi, G.; Sun, P.; Galvita, V.; Bell, A. T. Catalyst Performance of Novel Pt/Mg(Ga)(Al)O Catalysts for Alkane Dehydrogenation. *J. Catal.* **2010**, *274* (2), 200–206.
- (51) Liu, H.; Shen, W.; Bao, X.; Xu, Y. Methane Dehydroaromatization over Mo/HZSM-5 Catalysts: The Reactivity of MoC_x Species Formed from MoO_x Associated and Non-Associated with Brønsted Acid Sites. *Appl. Catal. A Gen.* **2005**, *295* (1), 79–88.
- (52) Yaragatti, R. M.; Malode, S. J.; Shetti, N. P.; Nayak, D. S.; Kulkarni, R. M.; Halbhavi, S. B.; Dandin, A. F.; Idli, D. C.; Kalmani, S. S.; Randewadi, V. A. *Chapter 9: Mass Spectrometry Chapter 14: HPLC*; **2019**; Vol. 18.

- (53) Kosinov, N.; Coumans, F. J. A. G.; Uslamin, E. A.; Wijpkema, A. S. G.; Mezari, B.; Hensen, E. J. M. Methane Dehydroaromatization by Mo/HZSM-5: Mono- or Bifunctional Catalysis? *ACS Catal.* **2017**, 7 (1), 520–529.